

# GIS-Based Landslide Susceptibility Map Verification by its Geotechnical and Geological Characteristics

Herianto, P.,\* Kunsuwan, B., Mairaing, W., Chalernpornchai, T. and Srisook, W.,

Division of Geotechnical Engineering, Department of Civil Engineering, Faculty of Engineering at Kamphaeng Saen, Kasetsart University, Kamphaeng Saen Campus, Thailand, E-mail: putra.h@ku.th

\*Corresponding author

## Abstract

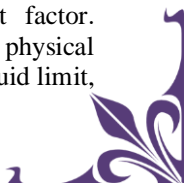
*The famous 2006 Laplae rainfall-triggered landslide has caused hundreds of million Baht lost. The objective of this paper is to evaluate and to compare present geotechnical and geological conditions between the landslide area and landslide-free area to verify a landslide susceptibility map. Detailed field surveys acquired 14 samples: undisturbed, disturbed soils as well as rocks. Sensitivity and back-analysis were also performed. 35.44% of landslides occurred in meta-shale - greywacke-interbedding Formation, and another 64.56% happened in meta-greywacke - basaltic andesite Formation. The dominant slope of the landslide is in 30<sup>o</sup>-40<sup>o</sup> slope, with aspects toward South direction, and in a range of <1,000 meters from geological structures. Landslide area is distinguished from the non-landslide area by its various grades of materials, lower quartz content, higher clay content, finer composition of parental rocks and soils, higher average ratio of smectite versus quartz, lower compressive strength, lower shear strength, lower angle of internal friction, lower cohesion value, more poorly graded, higher soil moisture, higher liquid limit and plasticity index, and factor of safety is generally less than 1. The result of the sensitivity analysis indicated that in a failure condition, the cohesion and angle of internal friction angle values are equal to 2.51 kPa and 13.70<sup>o</sup>, respectively. However, the results of laboratory tests showed that the cohesion and angle of internal friction values are equal to 8.59 kPa and 14.2<sup>o</sup>. These results verified the landslide susceptibility map that the high landslide susceptibility area has the engineering characteristics of the landslide-prone area, while the low susceptible one has the characteristics of the non-landslide area*

## 1. Introduction

A landslide is the movement of a mass of rock, debris, or earth down a slope under the influence of gravity (Guzzetti, 2005). Landslide hazard is one of the main natural disasters that need attention in Thailand. In 2006, two main landslide events caused a massive loss of both lives and properties in Uttaradit and Nan Provinces. When the Uttaradit Province landslide happened on 22-23 May 2006, the damaged cost was 308,615,331 Baht or roughly equal to 10 million US\$ (30 Baht = 1 US\$)(Usamah and Arambepola, 2013). The condition of this catastrophic translational landslides are shown in Figure 1. Laplae District is the most north-west district in Uttaradit Province (as shown in the Figure 2), where it was also swept away by the 2006 landslide. The lithology that composed of this study area is Greywacke, Shale, Claystone, and mixture of shale and volcanic ashes (Khositanont et al., 2016).

Many previous studies (Fell et al., 2008, 1994, Hwang et al., 2009 and Kim and Song, 2015) mentioned that the influencing factors on landslides could be divided into two groups. The first group is

related to fundamental factors, such as soil and rocks properties, geological structures, and topography, and the second group consists of external factors such as anthropogenic and rainfall intensity. Kim and Song (2015) explained that landslides might occur when the external factors, as a trigger, overlap with the inherent factors. For example, heavy rainfall may trigger landslides on an unstable clayey soil slope. Heavy rainfall, in this case, works as the external factor, while the unstable slope is the fundamental factor. The mentioned happened landslide in Uttaradit was mainly influenced by the rainfall and the physical properties of soil (Protong et al., 2018). The maximum rainfall intensity in May 2006 when the landslide occurred was 330.0 mm/day, and the limit for maximum rainfall intensity before the villagers need to evacuate is 150.0 mm/day (Mairaing et al., 2016). Similarly, like the previously mentioned case, the rainfall works as the external factor and the physical properties of soil work as the inherent factor. Several studies showed that particular physical properties, such as grading, unit weight, liquid limit,



and plasticity indexes, are noted as factors affecting slope stability as well (Fonseca et al., 2017, Kim and Song, 2015 and Mugagga et al., 2012). The physical properties of soil depend on the weathered grade and geology (Hurchinson, 1988, Lumb, 1975, Matsushi et al., 2006, Wakatsuki et al., 2005 and Yalcin, 2007). The characteristics of the weathered soil are derived from the characteristics of its parental rocks.

Living in the landslide-prone area means that the local people live in a high-risk area, especially when heavy downpours last for more than 24 hours like what happened in 2006. As this natural disaster frequently occurs in Laplae District, the geotechnical and geological conditions are the fundamental parameters that are scientifically and socially important. Several researchers did their research about the Laplae Landslide (Moazzam et al., 2007, Phattaraporn et al., 2017, Protong et al., 2018, Tanang et al., 2010 and Usamah and Arambepola, 2013) but none have ever done about using geological and geotechnical characteristics in order to verify the landslide susceptibility mapping of the area.

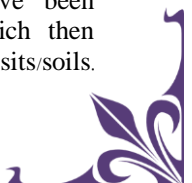
Herianto (2020) mentioned that they used the frequency ratio method in order to make the landslide susceptibility map, which has a range accuracy of the map from 49 to 89%. However, this accuracy verification was done by using area under curve and receiver operating characteristics curve, a statistical approach. Commonly, engineers prefer to validate further by using field and laboratory measurements to know whether the map that has been created is accurate enough based on physical field data. Herianto (2020) divided the landslide susceptibility map of Laplae area into five main landslide susceptibility index (LSI), as shown in Figure 3. The lower value of the LSI, meaning the lower probably a landslide will occur, while the higher the value of the LSI, meaning the higher probably a landslide will occur. Those five classes were subjectively renamed as very low susceptibility, low susceptibility, medium susceptibility, high susceptibility, and very high susceptibility.

However, the susceptibility maps formed was verified using only existing landslide location (scar data) by a statistical approach. In order to better understand and to verify the status of the landslide susceptibility map in the field, direct field and laboratory approaches will be done accordingly. The direct validation not only is important for increasing the susceptibility map precision, but its data can also be used for future landslide susceptibility modeling as input data, as shown in the flowchart of

methodology in Figure 4. This study not only evaluates and compares the geotechnical properties and geology of landslide locations but also works as an engineering verification of a landslide status in the GIS-based landslide susceptibility mapping of the area (Herianto, 2020) between the past location of landslides and landslide-free (or commonly called as non-landslide) location. Moreover, in order to compare and to evaluate these parameters on landslides, the properties of the soils that cover slopes are measured, and the geological conditions are investigated.

Three study areas are selected to consider and to validate different statuses of their historical landslide in 2006 based on scars data and previous researcher landslide susceptibility map (as shown in Figure 3). All of three chosen area (as shown in Figure 2 and 3) have different type of landslide status (based on the scar data and the previous researcher's landslide susceptibility map), which are a landslide area (very high susceptibility), a non-landslide area, and a non-landslide area close to the landslide area (low susceptibility). A detailed geotechnical and geological survey is performed as well as soil and rocks sampling in each study area. A series of laboratory soil tests are then conducted to measure the soil properties. Based on these results, the relationships between landslide occurrence and soil properties are investigated and evaluated, and the landslide susceptibility map will be well verified after the field verification is done. Hutchison (2014) agrees that Laplae is roughly located in the Sukhotai Zone, where it is bounded with Nan-Uttaradit Suture on the East part which extends on the North-South direction, Chiang Mai Suture on the West part which also extends from North to South, Mae Ping Fault on the South part which azimuth is trending from North- West to South-East and Ailao Shan-Red River Shear on the North part which also extends from North-West to South-East.

Khositanont et al., (2016) divided Laplae area into three different formations, geologically. There are Lower Lap-Lae Formation (Pli1), Upper Lap-Lae Formation (Pli2), and Alluvial Deposits (Qa). The Lower Lap-Lae Formation consists of meta-sandstone, greywacke, shale, and basaltic andesite sills. This Formation is called as Pli1. The Upper Lap-Lae Formation, on the other hand, consists of meta-shale or mudstone, greywacke sandstone, and mudstone. This Formation is called as Pli2. Geologically, those two Formations have been continuously weathered and eroded, which then become the source of the Quaternary deposits/soils.



The Alluvial Deposits consist of gravel, sand, silt, and clay. The age of this part is Quaternary, which is 0.01-1.6 Million years ago.

### 1.1 Study Sites

Ban Dee (BD) is in the North-East part of Mae Phun, Laplae District, Thailand, with elevation ranges between 200-500 m above sea level. Most of this area is still on their natural state, and even there are some cut roads established for local transportation, the vegetation dominated are natural trees with large and deep roots. This area was reported to be the less impacted area by the 2006

rainfall-triggered landslides. Huai Tong Sad (HTS) is in the Center part of Mae Phun, Laplae District, Thailand, with elevation ranges between 100-400 m above sea level. Most of this area is used for harvesting, the variation of productive trees dominantly are durian trees and langsat trees. There are also some parts of the area that are inhabited by local villagers' houses. This area was reported to be the most impacted area by the 2006 rainfall-triggered landslides. Not only be the most impacted area of landslide, but this area is also one of the most populated areas in Mae Phun.



Figure 1: The catastrophic Laplae landslide (Mairaing et al., 2016)

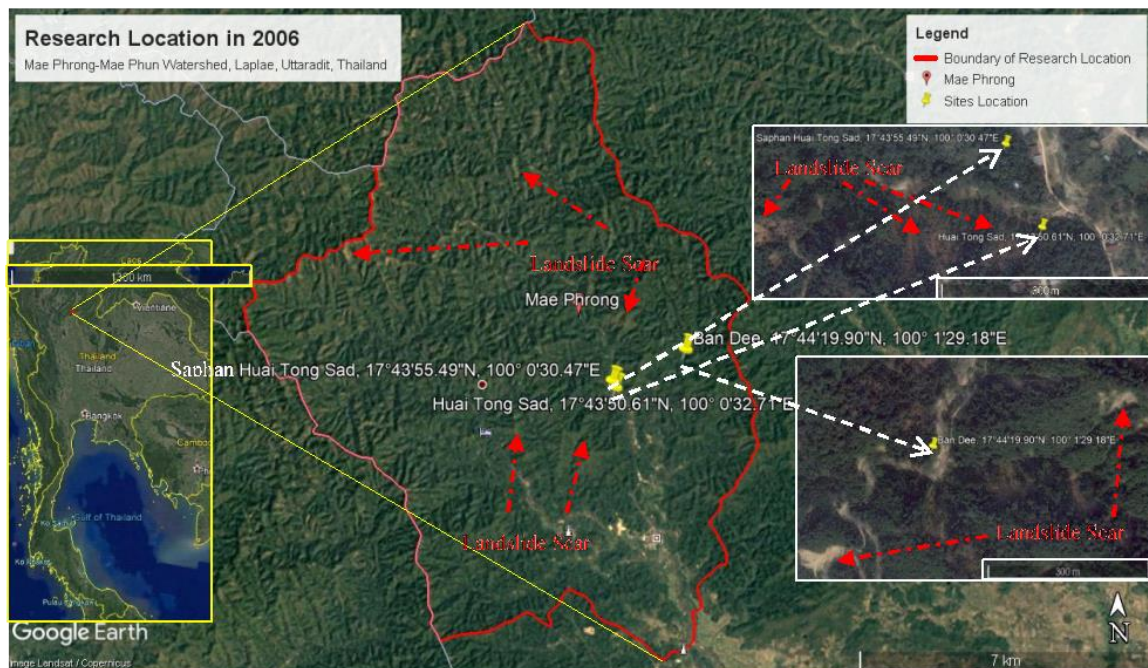


Figure 2: Research Location accessed in Google Earth



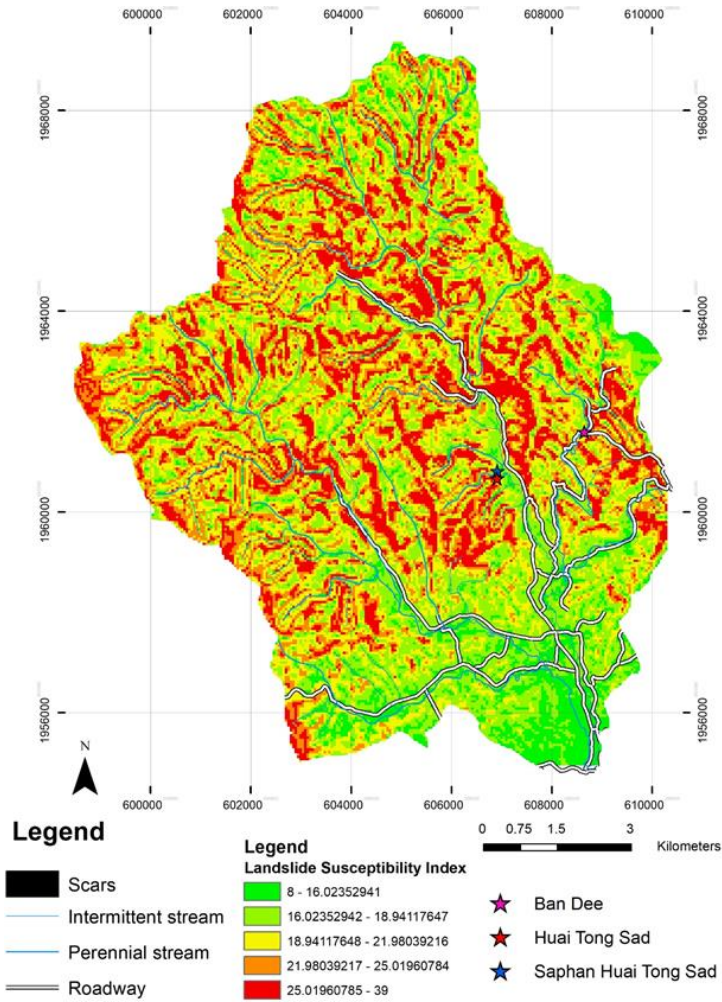


Figure 3: Landslide susceptibility index map of Mae Phun, Uttaradit, Thailand (Herianto, 2020)

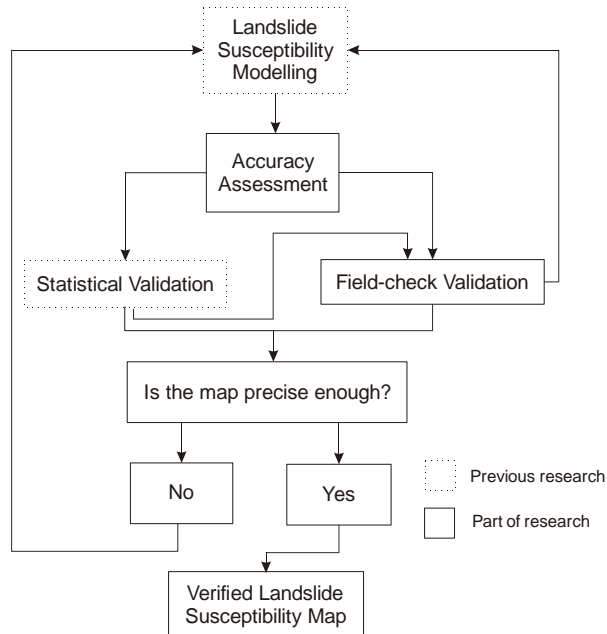


Figure 4: Methodology for landslide susceptibility mapping



Saphan Huai Tong Sad (SHTS) is located 200-meter North of the Huai Thong Sad site, with elevation ranges between 100-400 m above sea level. Most of this area is also being used for harvesting. This area, however, was reported to be less impacted area by the 2006 rainfall-triggered landslides. The anomaly of being next to the most impacted area of landslide despite not significantly impacted by a landslide is something that makes this area appealing to have a more in-depth investigation.

## 2. Methodology

### 2.1 Field Surveys

Field surveys entailed mapping the Laplae area using software such as Rockd (Wisconsin-Madison, 2019) and SuperSurv (Inc., 2019). A total of three sites was undertaken using a geological compass and a tape measure. At each point, pits were dug to a depth of 100 cm. Undisturbed soil samples were obtained at different depths (generally at an interval of 30 cm) using KU-miniature sampler, while disturbed soil samples were obtained at different depths of 30 cm also by using shovels. These samples were kept in air-tight-zipped plastic bags. Undisturbed soil samples were collected by using KU- miniature thin-wall sampler, developed by Kasetsart University (Mairaing et al., 2005), as shown in Figure 5a. These soil samples were used for the determination of cohesion and angle of internal friction under normal loading by conducting a multi-stage direct shear test in a consolidated drained test.

Not only soil samples that were taken, the rocks samples and geological structures were also obtained and identified by using geological compass by finding out strike/dip of the rock strata, rocks composition, and structures. Several field tests were conducted, such as pocket penetrometer (ASTM, 2010) for finding compressive strength and pocket shear vane (ASTM, 2019) to find the shear strength.

### 2.2 Laboratory Analyzes

In order to characterize and find out the physical properties of the slope materials in terms of its implications for slope stability, a series of analyzes were carried out at the Geotechnical Laboratory, Civil Engineering Department, Faculty of Engineering, Kasetsart University Kamphaeng Saen Campus. The analyzes focused on the particle-size distribution of soils, Atterberg limits, and shear strength. Petrography analysis was conducted in order to define the mineral composition of soil parental-rocks. Particle-size distribution test was conducted (ASTM, 2017c). The particle-size

distribution curve is used to calculate the coefficient of uniformity and the coefficient of concavity. Not only indicating their engineering properties, but the gradation of soil is also related to compressibility, friction angle, and shear strength (Islam et al., 2011 and Mostefa et al., 2013). The size of particles is directly proportional to the peak friction angle and angle of internal friction. The peak friction angle increases when the size of particles increases.

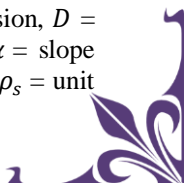
Atterberg limits are essential properties to point out soil expansion potential at different moisture and clay contents (Selby, 1993). Those properties explain the slope's susceptibility to various slope activities. The Atterberg's limits were determined (ASTM, 2017b). The higher clay content in the soil makes the higher PI in soil (Mugagga et al., 2012). Furthermore, the plasticity of the soils was further finalized using the unified soil classification system (USCS) in the plasticity chart, which also enabled further classification of the fine material. The multi-stage direct shear test uses a single soil specimen and shears the sample in stages with increasing normal stresses to minimize the testing sample (Mairaing et al., 2005). In addition, the multi-stage test is not an ASTM standard method for obtaining total or effective stress parameters but has been widely used in practice (Nam et al., 2011). Basically, the Mohr-Coulomb envelope is defined as the relationship of strength parameter ( $c'$ ,  $\phi'$ ). The three samples were tested in the conventional automatic direct shear test instrument, as shown in Figure 5b and 5c. This study applied a multi-stage direct shear test in order to find the shear strength of undisturbed samples. It was developed from a direct shear test. It is said that a multi-stage direct shear test is well suited for unsaturated soil testing where every single stage is tested until it is close to the failure point in each normal load (at least three or four normal loads) (Thongkhao et al., 2012).

After getting the strength parameters, cohesion, and angle of internal friction, those values then used to calculate the  $F_s$  of slopes. If the  $F_s$  is  $> 1$ , it means that the slope is inherently stable. However, it might fail by external factors causes. On the other hand, if the  $F_s$  is  $< 1$ , it means that the slope is naturally unstable (Berry and Reid, 1987). The  $F_s$  of an infinite slope is calculated by using Equation 1:

$$F_s = \left[ 1 - \frac{\rho_w}{\rho_s} \cdot \frac{D_w}{D} \right] \frac{\tan \phi}{\tan \alpha} + \frac{2C}{\rho_s g D \sin 2\alpha}$$

Equation 1

where  $D_w$  = depth of landslide,  $C$  = cohesion,  $D$  = slip depth,  $\phi$  = angle of internal friction,  $\alpha$  = slope angle,  $\rho_w$  = unit weight of water ( $1\text{g/cm}^3$ ),  $\rho_s$  = unit



weight of soil,  $g$  = gravitational acceleration ( $9.81 \text{ m/s}^2$ ). A back analysis is also done in order to compare the value of  $C$  and  $\phi$  from that with those obtained in the laboratory. The effect of  $C$  and  $\phi$  on the factor of safety was also given by doing the sensitivity analysis.

### 3. Results and Discussion

#### 3.1 Field Surveys and Mapping

The results from the field observations showed that, at the HTS landslide site, a translational debris flow had occurred. Evidence from past scars at the HTS site indicated an intermixture of materials between deeper depth materials and shallower materials. The SHTS site, however, was the non-landslide location. A further remote sensing analysis was also accomplished in order to verify landslide scars location by using a 15 m DEM, satellite image, and previous researchers' mapping results (Herianto, 2020 and Khositanont et al., 2016). The landslides were found to have occurred mostly on concave slopes ranging between 30-40 slope angles. The average depth of landslide is 2.3 meters, and the average depth of slip is 3 meters. The percentage of landslides that occurred in the meta-shale unit is 35.44%, while 64.56% happened in the meta-greywacke unit. Field measurements revealed that the compressive strength and the shear strength of the BD site, HTS site, and SHTS site, respectively, are 539 kPa and 54 kPa; 294 kPa and 44 kPa; 490 kPa and 49 kPa. It agrees with other researchers' results that the landslide area is having lower compressive strength and shear strength than the non-landslide area (Carruba and Moraci, 1993, Iannacchione and Vallejo, 2000 and Szafarczyk, 2019). The location has elevation ranges from 100 to 500 meters above sea level. The geomorphology of the sites is moderate-highly dissected denudational hills. The main lithology of the outcrops in location mostly consists of chert, siltstone, and sandstone.

The thickness of the outcrop in Figure 6 is approximately 3 meters. The color of the soils from chert is dark brownish-red. The grain size particle is  $<1/16 \text{ mm}$ , amorphous, layering structure, strike/dip  $N16^0E/55^0$ , mono-mineral silicas 100%, very low porosity. Total thickness is more than 5 meters. The thickness of the carbonaceous siltstone outcrop in Figure 7 is approximately 2 meters. The color of the soils of siltstone is brownish-red. The grain size particle is between  $1/256 \text{ mm}$  to  $>64 \text{ mm}$ , poorly sorted, sub-angular, matrix-supported. Lithic fragments consist of sandstone: whitish color, well-

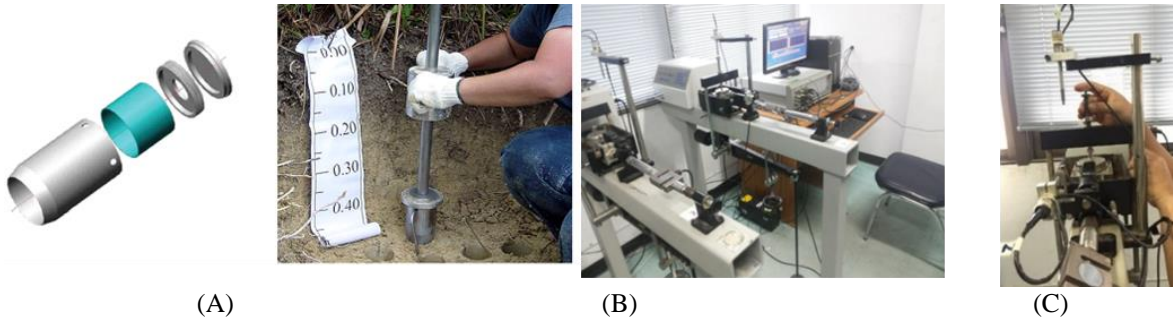
sorted,  $1/4 - 2 \text{ mm}$ , consist of 50% K-feldspar, 20% Ca/Na-Feldspar, 10% micas, 5% quartz and carbonates cement of 15%, massive, good porosity. Total thickness is more than 3 meters. The thickness of the carbonaceous sandstone outcrop in Figure 8 is approximately 5 meters. The color of the soils of sandstone is brownish-white. The grain size particle is between  $<1/16 \text{ mm}$  to  $2 \text{ mm}$ , well-sorted, sub-rounded, grain-supported. Lithic fragments consist of sandstone: whitish color, well-sorted,  $1/4 - 2 \text{ mm}$ , consist of 60% Ca/Na-feldspar, 20% K-Feldspar, 10% micas, 5% quartz and carbonates cement of 5%, massive, good porosity. Total thickness is more than 5 meters.

Strikes and dips, as well as lineaments in the location, are shown in Figure 9. These data are taken directly from the field. It is then combined with lithology, soils, and other topographic lineaments to make a geological map as well as to make a geological structure analysis. From the data, it shows that many lineaments of structures are controlling the research area. Most of the trend of the lineaments are elongated in the North-west South-east direction. From this data as well, faults and folds can be inferred based on the trend of structures, the trend of rivers direction, as well as contours elevation difference. The data of geological structures data, as shown in Figure 9, is then plotted and analyzed in the stereo net and the rose-net, as shown in Figure 10 and Figure 11. It shows from the rose-net analysis that the mean direction of the force comes from the North-West direction, which then makes folding that have North-East South-West folding plane direction. The mean direction of the fractures stress is  $N 342.6^0 E$ .

The geological map and the geological section of the research location is shown in Figure 12 and Figure 13, respectively. The units of geology in the location are divided into three different units. The oldest unit, which is part of PII1, is consisted of siltstone, in some places interbedded with sandstone and chert.

This unit is in green color on the map, which is called as Siltstone Interbedded with Sandstone and Chert Unit. The younger unit, which is part of PII2, is consisted of sandstone interbedded with chert. This unit is in yellow color on the map, which is called as Sandstone Interbedded with Chert Unit. The last unit, which is part of Qa, is consisted of alluvial deposits. This unit is in orange color on the map, which is called as Alluvial Deposits Unit.





(A) KU-miniature instrument (Mairaing, Thaijeamaree, & Kulsuwan, 2005), (B) the complete instruments of the direct shear test, and (C) the direct shear box equipment



Figure 6: An Outcrop in BD area

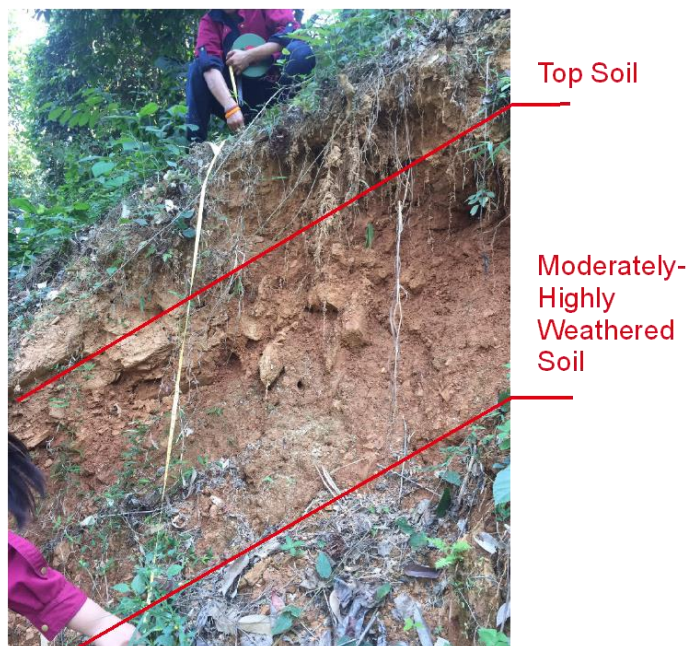


Figure 7: An Outcrop in HTS Area







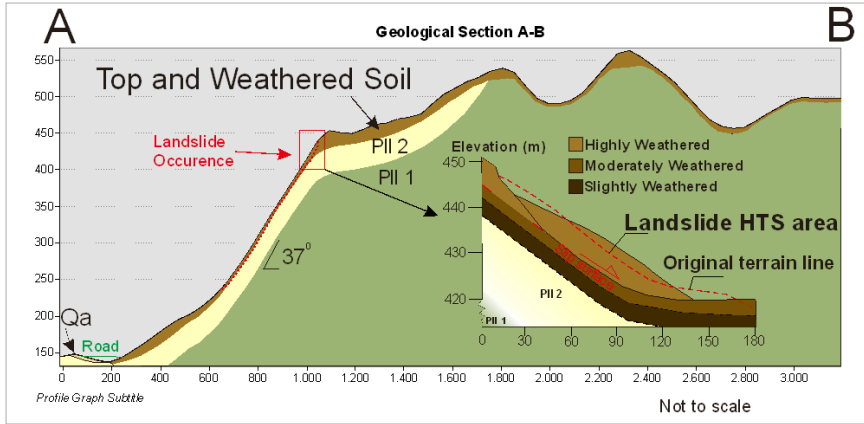


Figure 13: Geological section of laplae, Uttaradit, Thailand

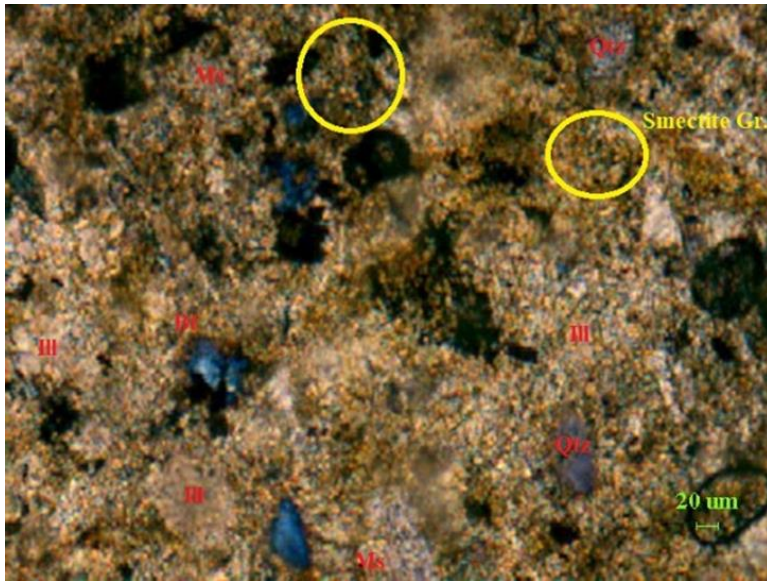


Figure 14: Shale thin section in the BD site under the normal-light microscope

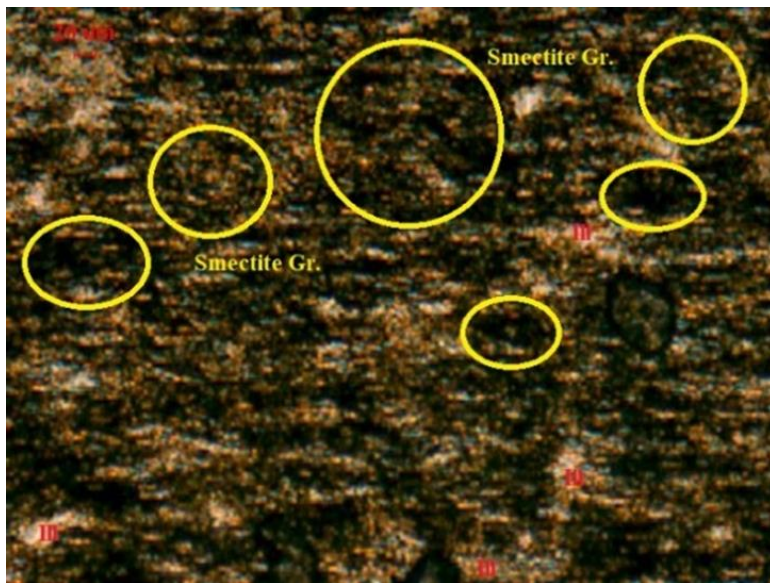


Figure 15: Siltstone thin section in the HTS site under the normal-light microscope



### 3.2 Petrography

Petrography analysis has been done by using a normal and cross-polarized microscope to show the mineral characteristics of soils' parental rocks in each site with point counting or modal composition method. The analysis is only focusing on the mineral quartz, smectite, and illite as these three minerals are the most common minerals found in the parental rocks' thin sections, while other minerals such as Plagioclase, Lithic Fragment, Muscovite and Biotite are quantitatively counted, but it has a less significant presence.

The average ratio of smectite vs. average of the other two minerals: quartz and illite, in each site, were also calculated. It shows that the average ratio of smectite with an average of quartz in HTS is 37.10, while on the other sites, it falls below 1.3. Moreover, the average ratio of smectite with an average of illite in HTS is 5.62, while on the other sites, it only reaches 0.32, as shown in Table 1. It means that smectite is the dominant minerals found to be the key mineral in the soil behavior in the landslide area, while illite is the dominant minerals in the non-landslide area. These results satisfy with other researchers' result that smectite is found to be the key minerals in the landslide area (Ohlmacher, 2001, Putra et al., 2019, Tamura and Hasegawa, 2015 and Zhao et al., 2007).

The results show that the highest mineral composition percentage in each site is different. Smectite is found to be the most abundant mineral in HTS site, as shown in Figure 15, while in BD and SHTS, as shown in Figure 14 and Figure 16, Illite is the most dominant mineral, as shown in Table 1. The result was also verified by the Department of Mineral Resources of Kingdom of Thailand which its laboratory analysis results show that the rocks found in BD, HTS, and SHTS sites are classified, respectively, as shale, siltstone, and sandstone.

### 3.2 Soil Particle Distribution

Particle distribution curves are shown in Figure 17. Soils from the respective sites were generally coarse-grained, with less than 50% of the material passing the 0.075 mm sieve.  $D_{60}$ ,  $D_{30}$  and  $D_{10}$  of the BD, HTS, and SHTS sites, respectively, are 5.50 mm, 2.00 mm, 0.40 mm; 2.00 mm, 0.80 mm, 0.40 mm; and 5.00 mm, 1.50 mm, 0.50 mm. Soils from the HTS site are finer and more poorly graded than those from the other two sites. The finer soil means that the angle of internal friction and the peak friction angle is lower, which leads to a weaker strength of soil which characterized the landslide area, as confirmed with other researchers' results

(Casini et al., 2011, Iannacchione and Vallejo, 2000, Islam et al., 2011, Mostefa et al., 2013 and Stark et al., 2014). Specifically, soils from BD site are greyish-brown gravelly sand, classified as well-graded sand with little fines material (SW), while HTS soils are reddish-brown silty sand, classified as poorly graded sand with little fines material (SP) groups. The soils from SHTS are yellowish-brown gravelly sand, classified as well-graded sand with little fines material (SW) groups.

### 3.3 Soil Moisture and Atterberg Limits

Soil moisture and Atterberg limits, as shown in Table 1, were measured and calculated for the behavior of soils in response to water content, and the following implications for landslide occurrence. Even though the soils are coarse-grained material, the Atterberg limits are calculated in order to analyze the behavior of the matrix-grained parts of the soil. The HTS soil has the highest soil moisture value. The liquid limit of HTS is above the threshold of 50% (ASTM, 2017a). It means that the HTS clay has high swelling potential of the clay materials. The PI of HTS site also shows the highest expansion potential of the clay materials among other sites as well, it is considered as high plasticity clays. This means that the nature of the soils might be one of the inherent factors. The plasticity chart, which including PI that highlights the range of water contents where the soil exhibits plastic properties, is shown in Figure 18. The plasticity chart shows that even though all the soils of the non-landslide area is critically near the 50% boundary of low and high plasticity, the only soil that contains high plasticity clay is located at HTS site. This confirms that the high plasticity of soils represents the characteristics of the landslide area as in accordance with others' results (Bizimana and Sönmez, 2015, Kitutu et al., 2009 and Soralump, 2008). The nature of highly plastic soil of HTS site is displayed by their plotting above the boundary A-line and their PI is exceeded the B-line threshold of 50%.

### 3.4 Shear Strength, $F_s$ and Sensitivity Analysis

The angle of internal friction and cohesion were computed by plotting shear strength versus normal stress curves, which were then used to calculate the Factor of Safety for each site. BD, HTS, and SHTS sites' curves are shown, respectively, in Figure 19(a,b,c). The number of points of scars vs. slope in the research area is shown in Figure 20. The landslides dominantly occurred in  $30^{\circ}$ - $40^{\circ}$  slope, with a mean of  $33.8^{\circ}$ .



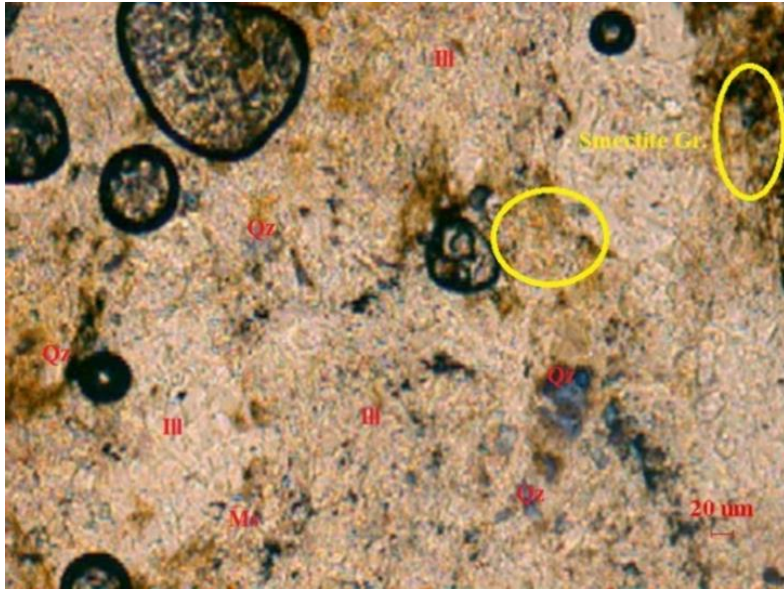


Figure 16: Sandstone thin section in the SHTS site under the normal-light microscope

Table 1: Laboratory analysis results

Properties	Fresh Rock-Slightly Weathered Soil (BD site)	Slightly-Moderately Weathered Soil (SHTS site)	Moderately-Highly Weathered Soil (HTS site)	
Gravels (%)	43.11	43.88	11.57	
Sand (%)	56.72	55.99	88.34	
Silt + Clay (%)	0.18	0.14	0.09	
USCS Classification	SW	SW	SP	
Specific Gravity	2.6	2.58	2.62	
LL (%)	49	49.70	55.2	
PL (%)	28.9	25.90	29.9	
PI (%)	20.1	23.80	25.3	
Optimum Water Content (%)	10.59	16.76	24.13	
Cohesion (kPa)	15.51	9.60	8.59	
Angle of Internal Friction (°)	27.22	25.26	14.2	
Average (%)	Quartz	14.67	2.22	27.78
	Smectite	18.22	82.44	14.89
	Illite	56.56	14.67	46.22
Average Clay Content (Smectite + Illite, %)	74.78	97.11	61.11	
Average Ratio Smectite : Average Quartz	1.24	37.10	0.54	
Average Ratio % Smectite : Average % Illite	0.32	5.62	0.32	
Mineral Composition	Illite Dominantly	Illite Dominantly	Smectite Group Dominantly	



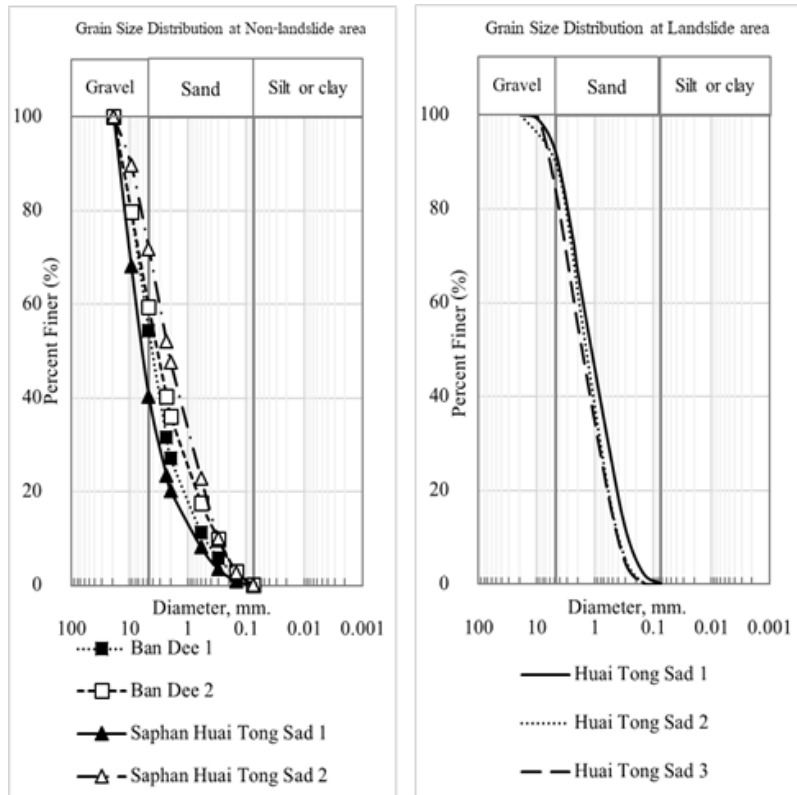


Figure 17: Particle distribution curve in the area

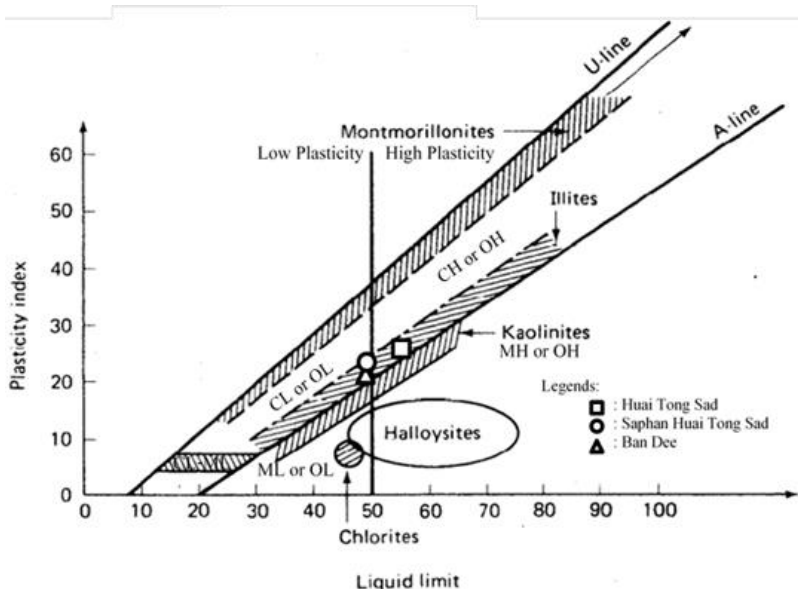


Figure 18: Casagrande plasticity chart of the site location (Modified from Holtz and Kovacs (1981))

As expected by the  $F_s$  calculation of infinite slope with various degree of slope, the slopes at BD and SHTS sites where the  $F_s > 1$ , tends to be more stable, while the slopes at the HTS site where the value of  $F_s$  is lower than the critical factor of 1, are unstable. However, this only applies at the slope angle of 32. The factor of safety also depends on the

slope angle of the area. When the slope angle of SHTS reaches 38, the  $F_s$  value falls below 1. It shows that even at the angle of 32 and 34, the slope at SHTS is still stable, but it becomes unstable when it reaches an angle of 38 or more. The HTS landslide occurred on naturally unstable, inherently expansive soils, harvested slopes.



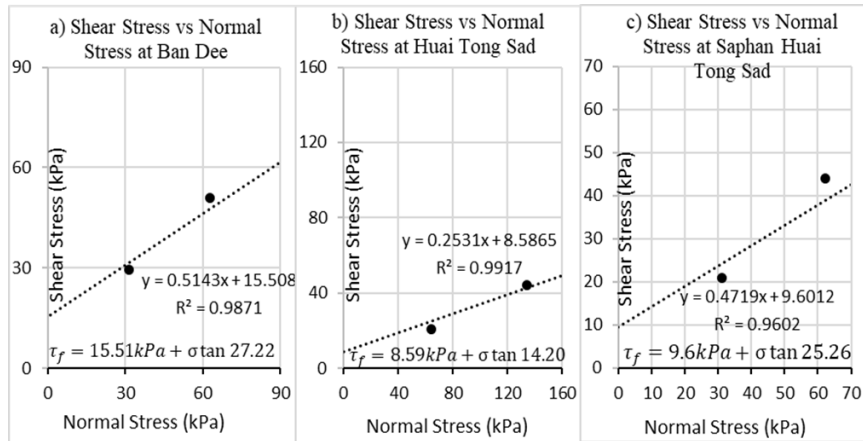


Figure 19: Shear stress versus normal stress curves for BD, HTS, and SHTS sites

Table 2: Factor of safety and strength parameters at the three sites

Dry density $g_b$ (g/cm <sup>3</sup> )	Slope Angle (°)	Cohesion C (kPa)	Angle of internal friction, $\phi$ (°)	Factor of safety
<b>Ban Dee</b>				
1.58	32	15.51	27.22	1.68
	34			1.58
	36			1.50
	38			1.42
	40			1.35
<b>Huai Tong Sad</b>				
1.51	32	8.59	14.20	0.93
	34			0.87
	36			0.83
	38			0.79
	40			0.75
<b>Saphan Huai Tong Sad</b>				
1.63	32	9.6	25.26	1.15
	34			1.08
	36			1.02
	38			0.97
	40			0.92

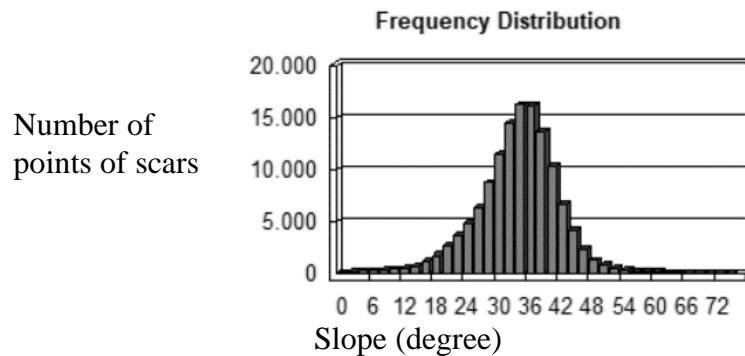


Figure 20: Frequency of landslide scars with various slope angle



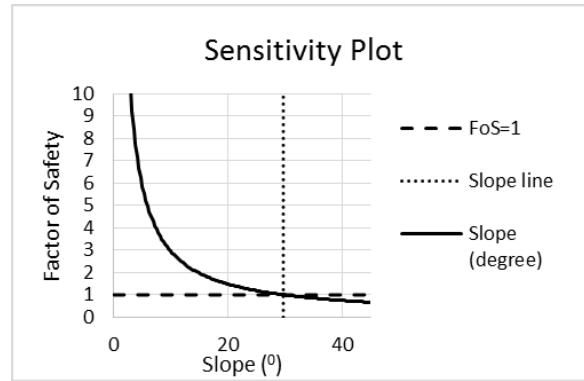


Figure 21: Sensitivity for slope

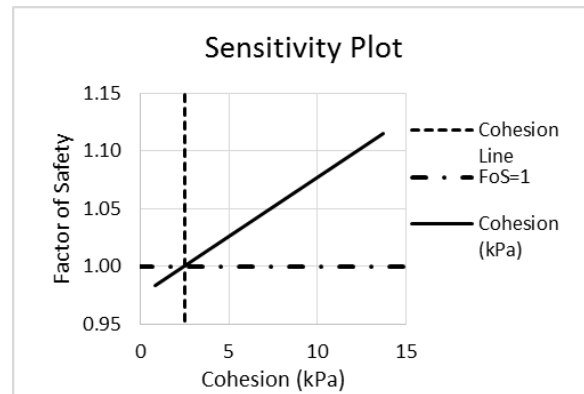


Figure 22: Sensitivity graph of cohesion

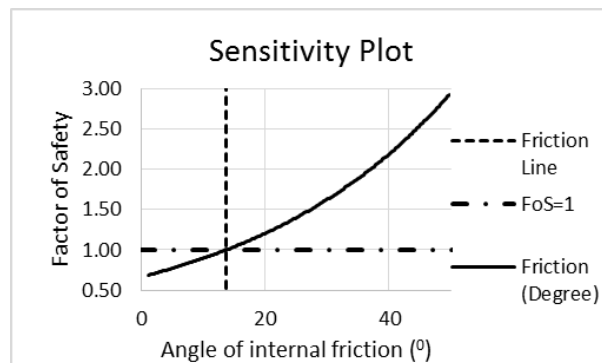
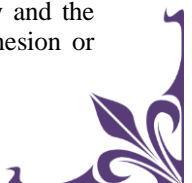


Figure 23: Sensitivity for friction angle

It needs to be noted that even slopes where  $F_s > 1$  is conditionally stable, the external and internal factors may change its stability when it applies their influence on landslides such as rainfall intensity rises, and the shrink-swell capacity of the clays triggered. These results also agree with other researchers' results, which show that translational failure mechanisms generally occurred at slopes with angles between  $8^\circ$  to  $32^\circ$  (Schilter, 2019), between  $30^\circ$  to  $45^\circ$  (Huang et al., 2016), more than  $25^\circ$  (Zêzere, 2002). Sensitivity analysis assists researchers to evaluate the impact of an individual unknown variable, with the assumption that all other slope parameters are known. In this analysis, one

parameter varies, and other input parameters are kept constant in their mean values. The analysis assesses of which input parameter may be more critical to the assessment of the slope stability, and vice versa, which parameter has less effect on the instability. The cohesion and friction angle of the failure surface was back analyzed by performing a sensitivity analysis. The effects of slope, cohesion, and angle of internal friction to the factor of safety are presented in the form of sensitivity graphs in Figure 21, Figure 22, and Figure 23 in which the vertical axis represents the factor of safety and the horizontal axis represents the slope or cohesion or angle of internal friction.



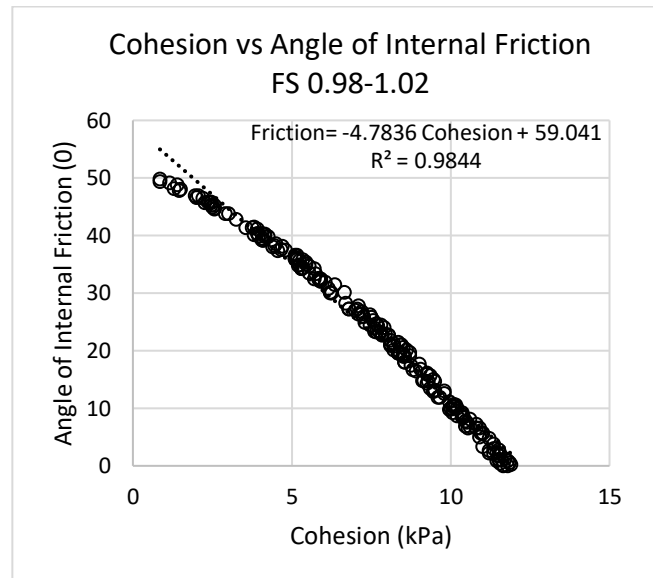


Figure 24: The relationship between cohesion and friction angle of the rock mass for an approximate factor of safety of 1, the dotted line is the line of factor of safety = 1

The value of cohesion and angle of internal friction by using the back analysis is compared with the value of cohesion and angle of internal friction obtained from the laboratory. The slope, cohesion, and the angle of internal friction obtained in the laboratory of the HTS site, where a landslide did occur in 2006, is  $30^{\circ}$ , 8.59 kPa and  $14.2^{\circ}$ , respectively. On the other hand, from the back-analysis result, it is indicated that at the edge of failure, i.e., a factor of safety of 1, the slope, cohesion, and friction angle values were  $29.63^{\circ}$ , 2.51 kPa and  $13.70^{\circ}$ , respectively. The relationship of cohesion and angle of internal friction from the back analysis is shown in Figure 24.

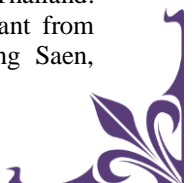
#### 4. Conclusions

The GIS-based landslide susceptibility map is now field, and laboratory-verified that the high landslide susceptibility area has the engineering characteristics of the landslide-prone area, while the low susceptible one has the characteristics of the non-landslide area. High susceptibility landslide area is characterized by the intermixture of materials of deep and shallow materials, lower quartz content, higher clay content (especially smectite group clay), finer composition of parental rocks and soils, higher average ratio of smectite vs. quartz, lower compressive strength, lower shear strength, lower angle of internal friction, lower cohesion value, more poorly graded, higher soil moisture, higher liquid limit and plasticity index, with the slope angle between  $30^{\circ}$  to  $40^{\circ}$  and factor of safety is generally less than 1. Vice versa, low susceptibility landslide area is characterized by more homogenous

materials, higher quartz content, lower clay content, more grainy composition of parental rocks and soils, lower average ratio of smectite vs. quartz, higher compressive strength, higher shear strength, higher angle of internal friction, higher cohesion value, more well-graded, lower soil moisture, lower liquid limit and plasticity index, and factor of safety is generally more than 1. The factor of safety of SHTS area, however, falls below 1 once the slope angle reaches  $38^{\circ}$ . The result of the sensitivity analysis indicated that in a failure condition, the cohesion and angle of internal friction angle values are equal to 2.51 kPa and  $13.70^{\circ}$ , respectively. However, the results of laboratory tests showed that in a failure condition, the cohesion and angle of internal friction values are equal to 8.59 kPa and  $14.2^{\circ}$ . In a nutshell, the hypothesis that geological and geotechnical properties as the inherent factors are related to the landslide occurrence at the site where the slope failure occurred, is now generally accepted.

#### Acknowledgments

This research was funded by Kasetsart University Postgraduate Scholarship Program for ASEAN Students 2017, Kasetsart University Scholarships for ASEAN for Commemoration of the 60th Birthday Anniversary of Professor Dr. Her Royal Highness Princess Chulabhorn Mahidol, grant number 1/2560. This research was also supported by the Department of Civil Engineering, Faculty of Engineering at Kamphaeng Saen, Kasetsart University, Kamphaeng Saen Campus, Thailand. This research was also supported by a grant from the Faculty of Engineering at Kamphaeng Saen,



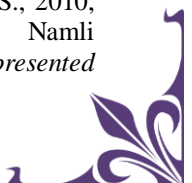
Kasetsart University, Kamphaeng Saen Campus, Thailand. The author would like to thank the reviewers.

## References

- ASTM, 2010, *New Test Method for Pocket Penetrometer Test*. In ASTM WK27337. West Conshohocken, PA: ASTM International.
- ASTM, 2017a, *Standard Practice for Classification of Soils for Engineering Purposes (Unified Soil Classification System)*. In ASTM D2487-17. West Conshohocken, PA: ASTM International.
- ASTM, 2017b, *Standard Test Methods for Liquid Limit, Plastic Limit, and Plasticity Index of Soils*. In ASTM D4318-17e1. West Conshohocken, PA: ASTM International.
- ASTM, 2017c, *Standard Test Methods for Particle-Size Distribution (Gradation) of Soils Using Sieve Analysis*. In ASTM D6913 / D6913M-17. West Conshohocken, PA: ASTM International.
- ASTM, 2019, *Standard Test Method for Approximating the Shear Strength of Cohesive Soils by the Handheld Vane Shear Device*. In ASTM D8121 / D8121M-19. West Conshohocken, PA: ASTM International.
- Berry, P. L. and Reid, D., 1987, *An Introduction to Soil Mechanics*: McGraw-Hill.
- Bizimana, H. and Sönmez, O., 2015, Landslide Occurrences in the Hilly Areas of Rwanda, their Causes and Protection Measures. *Disaster Science and Engineering*, Vol. 1(1), 1-7.
- Carruba, P. and Moraci, N., 1993, Residual Strength Parameters from a Slope Instability. *Proceedings Third International Conference on Case Histories in Geotechnical Engineering, St. Louis*. 1481-186.
- Casini, F., Brauchli, S., Herzog, R. and Springman, S. M., 2011, Grain Size Distribution and Particle Shape Effects on Shear Strength of Sand- Gravel Mixtures. *Paper presented at the 15th European Conference on Soil Mechanics and Geotechnical Engineering (XV ECSMGE)*. <http://hdl.handle.net/20.500.11850/39588>.
- Fell, R., 1994, Stabilization of Soil and Rock Slopes. Paper presented at the Proc. East Asia Symp. and Field Workshop on Landslides and Debris Flows, Seoul.
- Fell, R., Corominas, J., Bonnard, C., Cascini, L., Leroi, E. and Savage, W. Z., 2008, Guidelines for Landslide Susceptibility, Hazard and Risk Zoning for Land-Use Planning. *Engineering Geology*, Vol. 102(3), 99-111. doi:<https://doi.org/10.1016/j.enggeo.2008.03.014>
- Fonseca, L., Luiz Lani, J., Fernandes Filho, E., Santos, G., Ferreira, W. and Maria Rocha Trancoso Santos, A. (2017). Variability in Soil Physical Properties in Landslide-Prone. *Acta Sci., Agron.*, Vol. 39, No.1.
- Kitutu, M. G., Muwanga, A., Poesen, J. and Deckers, J. A., 2009, Influence of Soil Properties on Landslide Occurrences in Bududa District, Eastern Uganda. *African Journal of Agricultural Research*, Vol. 4, 611-620.
- Guzzetti, F., 2005, *Landslide Hazard and Risk Assessment: Concepts, Methods and Tools for the Detection and Mapping of Landslides, for Landslide Susceptibility Zonation and Hazard Assessment, and for Landslide Risk Evaluation*. (ERLANGUNG DES DOKTORGRADS (DR. RER. NAT.)). RHEINISCHEN FRIEDRICH-WILHELMS-UNIVESTITÄT BONN,
- Herianto, P., 2020, *Landslide Susceptibility Mapping by Integrating Multidisciplinary Data*. (Master of Engineering). Kasetsart University Kamphaeng Saen Campus, Thailand.
- Holtz, R. D. and Kovacs, W. D., 1981, *An Introduction to Geotechnical Engineering: Prentice-Hall*. Presses Internationales Polytechnique.
- Huang, W., Leong, E. and Rahardjo, H., 2016, Governing Failure Mode of Unsaturated Soil Slopes Under Rainwater Infiltration. *E3S Web of Conferences*, 9, 15008. doi:10.1051/e3sconf/20160915008.
- Hurchinson, J., 1988, *General report: Morphological and Geotechnical Parameters of Landslides in Relation to Geology and Hydrology*. Paper presented at the V International Symposium on Landslides, Lausanne. 3-35.
- Hutchison, C. S., 2014, Tectonic Evolution of Southeast Asia. *Bulletin of the Geological Society of Malaysia*, Vol. 60, 1-18.
- Hwang, S., Guevarra, I. F. and Yu, B., 2009, Slope Failure Prediction Using a Decision Tree: A Case of Engineered Slopes in South Korea. *Engineering Geology*, Vol. 104(1), 126-134. doi:<https://doi.org/10.1016/j.enggeo.2008.09.004>
- Iannacchione, A. T. and Vallejo, L. E., 2000, Shear Strength Evaluation of Clay-Rock Mixtures. *In Slope Stability 2000*. 209-223.
- Inc., S. T., 2019, SuperSurv (Version 10.0.0001) [iPhone software]: Supergeo Technologies Inc.
- Islam, M., Siddika, A., Hossain, M., Rahman, A. and Asad, M. A., 2011, Effect of Particle Size on the Shear Strength Behaviour of Sands. *Australian Geomechanics Journal*, Vol. 46, 85-95.



- Khositanont, S., Wattanapradtha, S., Kunttasub, P., Suthisook, T., Dampitak, S., Nilda, K., Kaewmanee, P., and Pacca, I. (2016). The Study On Geological Environments and Rainfall in Relation to the Effect of Landslide. Research and Development for Landslide Protection on Highland Slope Project Under the King Initiation (Chaipattana Foundation).
- Kim, K.-S. and Song, Y.-S., 2015, Geometrical and Geotechnical Characteristics of Landslides in Korea Under Various Geological Conditions. *Journal of Mountain Science*, Vol. 12(5), 1267-1280.
- Lumb, P., 1975, Slope Failures in Hong Kong. *Quarterly Journal of Engineering Geology and Hydrogeology*, Vol. 8(1), doi:10.1144/GSL.QJEG.1975.008.01.02
- Mairaing, W., Thaijeamaree, N. and Kulsuwan, B., 2005, *Landslide study in Phetchabun and Chanthaburi*. (Kasetsart University).
- Mairaing, W., Thaiyuenwong, S., Kulsuwan, B., Chantasorn, M., Pitayaniwit, J., Akejit, M., Butam, P., and Phumchaem, S. (2016). Geotechnical Engineering Modelling for Prediction of Landslide Prone Area. Research and Development for Landslide Protection on Highland Slope Project Under the King Initiation (Chaipattana Foundation).
- Matsushi, Y., Hattanji, T. and Matsukura, Y., 2006, Mechanisms of Shallow Landslides on Soil-Mantled Hillslopes with Permeable and Impermeable Bedrocks in the Boso Peninsula, Japan. *Geomorphology*, Vol. 76(1), 92-108. doi:https://doi.org/10.1016/j.geomorph.2005.10.003.
- Moazzam, M. F. U., Vansarochana, A., Boonyanuphap, J. and Choosumrong, S., 2017, *Landslide Assessment Using Gis-Based Frequency Ratio Method: A Case Study of Mae-Phun Sub-District, Laplae District, Uttaradit Province, Thailand*. Paper presented at the 38th Asian Conference on Remote Sensing (ACRS 2017), Delhi.
- Mostefa Kara, E., Meghachou, M. and Aboubekr, N., 2013, Contribution of Particles Size Ranges to Sand Friction. *ETASR - Engineering, Technology & Applied Science Research*, Vol. 3(4), 5.
- Mugaga, F., Kakembo, V. and Buyinza, M., 2012, A Characterisation of the Physical Properties of Soil and the Implications for Landslide Occurrence on the Slopes of Mount Elgon, Eastern Uganda. *Natural Hazards*, Vol. 60(3), 1113-1131. doi:10.1007/s11069-011-9896-3.
- Nam, S., Gutierrez, M., Diplas, P. and Petrie, J., 2011, Determination of the Shear Strength of Unsaturated Soils Using the Multistage Direct Shear Test. *Engineering Geology*. Vol. 122(3-4), 272-280.
- Ohlmacher, C.G. 2001. The Relationship Between Geology and Landslide Hazards of Atchison, Kansas, and Vicinity. Current Research in *Earth Sciences*, 244.
- Phattaraporn, S., Anusorn, R. and Thitawadee, S., 2017, *Analyzing the Effects of Land Use changes for Landslide Susceptibility Assessment: A Case Study of LabLae district, Uttaradit province, Thailand*. Paper presented at the 38th Asian Conference on Remote Sensing (ACRS 2017), Delhi.
- Protong, S., Carling, P. A. and Leyland, J., 2018, Climate Change and Landslide Risk Assessment in Uttaradit Province, Thailand. *Engineering Journal*, Vol. 22(1), 243-255. doi:10.4186/ej.2018.22.1.243.
- Schilter, J., 2019, *Identifying Key Factors Affecting Translational Landslides in Part of the Yakima Fold and Thrust Belt, Washington State (Master of Science (MS))*. Central Washington University,
- Selby, M. J., 1993, *Hillslope Materials and Processes / M.J. Selby; with a Contribution by A.P.W. Hodder*. Oxford, England: Oxford University Press.
- Soralump, S., 2008, Landslide Hazard Investigation Aand Evaluation of Doi Tung Palace: Example of soil Creep Landslide. *Paper Presented at the EIT-JSCE Joint International Symposium "Monitoring & Modelling in Geo-Engineering Bangkok, Thailand*.
- Stark, N., Hay, A. E., Cheel, R. and Lake, C. B., 2014, The Impact of Particle Shape on the Angle of Internal Friction and the Implications for Sediment Dynamics at a Steep, Mixed Sand-Gravel Beach. *Earth Surf. Dynam.*, Vol. 2(2), 469-480. doi:10.5194/esurf-2-469-2014.
- Szafarczyk, A., 2019, Stages of Geological Documentation on the Example of Landslides Located on the Slopes of the Dam Reservoir "Swinna Poreba" (Poland). *IOP Conference Series: Earth and Environmental Science*, 221, 012037. doi:10.1088/1755-1315/221/1/012037.
- Tamura, E. and S. Hasegawa (2015). *Verification of swelling and landslides of smectite-bearing ground due to hydrothermal alteration in non-volcanic region*. 10th Asian Regional Conference of IAEG. Kyoto, Japan.
- Tanang, S., Sarapirome, S. and Plaiklang, S., 2010, Landslide Susceptibility Map of Namli Watershed, Uttaradit, Thailand. *Paper presented*



- at the 31st Asian Conference on Remote Sensing 2010.
- Thongkhao, T., Choowong, M., Charusiri, P. and Thitimakorn, T., 2012, *Engineering Properties of Residual Soil from Landslide Hazard Area in Ban Nong Pla Village, Chiang Klang District, Nan Province*, Northern Thailand. Bulletin of Earth Sciences of Thailand.
- Usamah, M. and Arambepola, N., 2013, Lessons Learned from the 2006 Flashfloods and Landslide in Uttaradit and Sukhothai Provinces: Implication for Effective Landslide Disaster Risk Management in Thailand. *Landslide Science and Practice*, Vol. 6. doi:10.1007/978-3-642-31319-6\_88.
- Wakatsuki, T., Tanaka, Y. and Matsukura, Y., 2005, Soil Slips On Weathering-Limited Slopes Underlain by Coarse-Grained Granite or Fine-Grained Gneiss Near Seoul, Republic of Korea. *CATENA*, Vol. 60(2), 181-203. doi:<https://doi.org/10.1016/j.catena.2004.11.003>.
- Wisconsin-Madison, U., 2019, Rockd (Version 2.6.0) [iPhone software]: UW Board of Regents, 2019.
- Yalcin, A., 2007, The Effects of Clay on Landslides: A Case Study. *Applied Clay Science*, Vol. 38(1), 77-85. doi:<https://doi.org/10.1016/j.clay.2007.01.007>.
- Zhao, Y., et al. 2007. *Evolution of Shear Strength of Clayey Soils in a Landslide Due to Acid Rain: A Case Study in The Area of Three Gorges, China*. First North American Landslide Conference, Landslides and Society: Integrated Science, Engineering, Management, and Mitigation. Vail, Colorado.
- Zêzere, J. L., 2002, Landslide Susceptibility Assessment Considering Landslide Typology. A Case Study in the Area North of Lisbon (Portugal). *Nat. Hazards Earth Syst. Sci.*, Vol. 2(1/2), 73-82. doi:10.5194/nhess-2-73-2002.

